[10]H. Kendrick, A. Arrott, and S. A. Werner, J. Appl. Phys. 39, 585 (1968).
[11]D. Adler, in *Solid State Physics*, edited by F. Seitz, D. Turnbull, and H. Ehrenreich (Academic, New York, 1968), Vol. 21, p. 1.
[12]B. I. Halpern and T. M. Rice, Rev. Mod. Phys. 40, 755 (1968); D. Jerome, T. M. Rice and W. Kohn, Phys. Rev. 158, 462 (1967).
[13]D. Adler and H. Brooks, Phys. Rev. 155, 826 (1967).
[14]T. Matsubara and T. Yokota, in *Proceedings of the International Conference on Theoretical Physics, Kyoto and Tokyo*, 1953 (Science Council of Japan, Tokyo, 1954), p. 693.
[15]N. F. Mott, Proc. Phys. Soc. (London) A62, 416 (1949).
[16]A preliminary version of this model was presented by L. M. Falicov and J. C. Kimball, Phys. Rev. Letters 22, 997 (1969).
[17]R. L. Cohen, M. Eibschütz, and K. W. West, Phys. Rev. Letters 24, 383 (1970).
[18]A similar model with itinerant holes in the valence band and localized electrons such that the ion goes from the nth state of ionization in the insulating phase to $(n-1)$th state in the metallic phase can be equally acceptable. For the sake of definiteness, we restrict ourselves to localized holes and itinerant electrons.
[19]C. E. Moore, *Atomic Energy Levels* (Natl. Bur. Std., Washington, D. C., 1949), Vol. 1.
[20]Since the number of electrons is equal to the number of holes, the electron-electron interaction can be equally well taken into account in the model; this is equivalent to replacing in Eqs. (2.6) G_4 by G, which is the difference between an effective electron-hole interaction and an electron-electron average interaction. $|G| \approx |G_4| - |\bar{G}_6|$.
[21]G. N. Watson, Quart. J. Math. 10, 266 (1939).
[22]Figures 4–8 are all shown, for the sake of consistency, in the same scale. Figure 7 only shows a jump in n_T by about a factor of 3. It is, however, possible, by properly changing G, to make that jump as large as desired, including a value of 10^8 found experimentally for V_2O_3 (Fig. 1).
[23]J. Ziman, *Electrons and Phonons* (Oxford U. P., London and New York, 1960); J. F. Blatt, in Ref. 11, Vol. 4, p. 200.
[24]J. Kondo, Progr. Theoret. Phys. (Kyoto) 32, 37 (1964).
[25]A. Jayaraman, Phys. Rev. 137, A179 (1965).

PHYSICAL REVIEW B VOLUME 2, NUMBER 8 15 OCTOBER 1970

Thermally Stimulated Conductivity and Luminescence in KBr Due to γ Irradiation at 10°K

W. Fuchs* and A. Taylor†
Department of Materials Science and Engineering, Cornell University, Ithaca, New York 14850
(Received 9 March 1970)

The annealing behavior of KBr, γ-irradiated at 10 °K, was studied by means of simultaneous measurements of the thermally stimulated conductivity and luminescence and of the optical absorption. Over the investigated temperature range between 10 and 35 °K, the conductivity and luminescence behaved very similarly, and the latter did not change its spectral distribution. All observed peaks have been ascribed to the annealing of the irradiation-induced imperfections of the lattice structure. Four peaks, appearing at 14, 17, 20, and 24 °K with characteristic activation energies between 0.025 and 0.058 eV, which saturate in intensity after a moderate irradiation dose, are believed to be due to the generation of conduction electrons. A smaller peak at 22 °K, which was observed only in the conductivity data, may be due to ionic motion. The most prominent peak appeared at 27 °K, and it was shown by "thermal cleaning" experiments that this peak is caused by processes with activation energies of 0.062 and 0.100 eV. Here, too, the signals are believed to be caused by conduction electrons and their consecutive recombination with traps. The 0.062-eV process has "mixed-order" kinetics, i.e., there is an excess of recombination centers. At higher irradiation doses, the 0.100-eV process becomes dominant. This process seems to be associated with the first annealing stage of the H band, which had an activation energy of 0.097 eV. A tentative model of the H-center decay involves the dissociation of the H center followed by an interstitial-vacancy recombination.

I. INTRODUCTION

It is generally believed that the low-temperature annealing processes of the interstitial-type centers in irradiated KBr crystals are associated with the recombination of complimentary centers. Considerable light on the nature of the annealing of the Br^- interstitial has come from the kinetic studies of the α-band annealing carried out by Smoluchowski and his co-workers.[1,2] In particular, these workers suggest that the annealing event at 22 °K is due to a random migration of Br^- interstitials with a motion

energy of 0.06 eV. At slightly higher temperatures (≈ 26 °K), approximately 25% of the composite "*H*" optical absorption is annealed with a corresponding reduction in the height of the *F* band. As yet, however, no kinetic studies have been carried out on this event. During an investigation of neutron- and γ-irradiation-induced defects in KBr,[3] we have been led to study the annealing of the *H* center in some detail. Because of the need to compare the neutron and γ-irradiation results at similar dosages, the present work has been carried out at comparatively low defect concentrations [$\gtrsim 10^{16}$ (*F* centers)/cm^3]. The experimental approach of Dutton and Maurer[4] was employed. These workers compared simultaneous measurements of thermally stimulated luminescence (TSL) and thermally stimulated conductivity (TSC) with changes in the optical-absorption spectra. However, in order to obtain detailed quantitative information on the kinetics of the annealing process the basic technique was improved so that the crystal temperature could be accurately determined. The data presented here cover the temperature range from 10 °K to 30 °K. Similar data for annealing between 30 °K and 300 °K will be presented elsewhere.

II. EXPERIMENTAL PROCEDURE

A set of KBr single crystals were exposed to γ irradiation at 10 °K. Subsequently, they were warmed up simultaneously at a constant rate, while the electrical conductivity and the luminescence of the crystals were measured and recorded. Also the optical absorption was observed with a special attention to the *H* band (380 nm).

A. Sample Chamber

For practical reasons, the various quantities were measured on separate samples. In order to optimize the uniformity of the temperature distribution the crystals were arranged in a sample chamber containing He gas at atmospheric pressures as shown in Fig. 1. Three windows of quartz glass facilitated the measurements. The optical absorption was measured on a crystal with dimensions of 1.3×1.3× 5.7 cm^3 with the light beam directed along the long dimension. This long light path was necessary due to the small defect concentrations. The luminescence was observed on a separate piece with a thickness of 0.5 cm, and occasionally also on the optical crystal. The conductivity was measured independently on two crystals with a thickness of less than 2 mm. Silver electrodes were painted on the large faces of ~ 2 cm^2 on both sides. One side of each crystal was connected to a 300-V battery. The connections to the electrometer were made through the bottom plate of the sample chamber using stycast 2850 GT (Emerson and Cumings, Inc.) feed throughs.

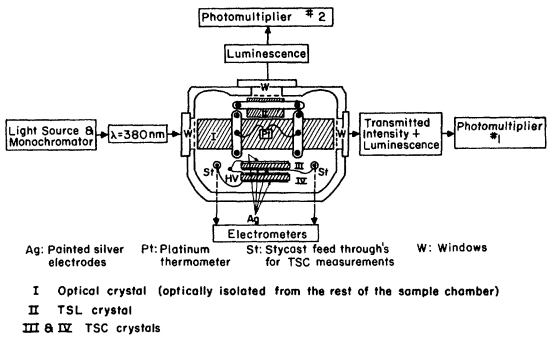

FIG. 1. Schematic representation of the cryostat sample chamber.

B. Temperature Control

The temperature was monitored by a Rosemount platinum resistance thermometer type 118L attached to the large crystal. The nominal accuracy was 0.04 °K. A heating rate of approximately 0.01 °K/sec was applied using a programmer and electronic controller.[3] The heating units (two 50-W Zener diodes) and a control thermometer (a second Rosemount unit) were attached to the copper plate serving as heat exchanger between the sample chamber and the exchange gas chamber. Slow variations of the heating rate, which could not be avoided at lower temperatures, were given consideration in the data analysis. Statistical fluctuations about the average rate were less than 0.005 °K/sec. It was found that the behavior of the glow curves and of the conductivity is not influenced by the size of the crystals nor by their position within the sample chamber. This is sufficient proof that the temperature is uniformly distributed among the crystals and within the larger crystals.

C. Detectors

The TSC's were measured by two Cary vibrating reed electrometers. The electrical connections had to be made rather rigid to minimize the noise. By carefully mounting the electrometer and avoiding any mechanical vibrations the background noise of the recorded conductivity could be kept below 5×10^{-19} Ω^{-1} cm^{-1}. The average precision obtained was 0.05%, the accuracy was ~ 10%. The peaks could be reproduced rather well with respect to their shape. A slight fluctuation of the peak temperature of 0.1 °K (between runs but under identical irradiation conditions) is probably ascribable to variations in the heating rate. The peak intensities agreed within 30%. The response time of the current detection system could not be neglected.

It is, however, not affected by the dielectric properties of the probe, therefore, one could correct for it in the final analysis in a straightforward manner. This correction was tested by using in one run two different time constants (11 and 66 sec) for the two electrometers.

For the TSL, 1P28 photomultiplier tubes were used. When no absorption was measured the TSL was observed through two windows, one of which was covered by a Corning glass filter (2-73), which eliminated all wavelengths shorter than 4750 Å. The photocathodes and the dynodes of the phototubes were cooled by keeping the pins at the metal-to-glass seals at dry-ice temperature. This kept the dark current down below 10^{-9} A with a noise level of 10^{-10} A. Therefore, every signal larger than 10^{-10} A, which corresponds to 10^3 incident photons per second, could be detected. The reproducibility of the signal height for repeated runs was somewhat limited by errors in repositioning the phototube subsequent to the irradiation. Exposure of the photomultiplier tubes to the high irradiation levels was considered undesirable. In most cases the reproduced signals agreed within 40%. In contrast, the curve shapes and peak temperatures agreed well with each other and were in a systematic correlation with the TSC data.

The optical-absorption data were taken with a Cary 14R spectrophotometer. For a continuous recording of the optical density at 380 nm, a Bausch and Lomb grating monochromator with a tungsten filament lamp was used as a light source and the transmitted intensity was measured with a 1P28 photomultiplier tube.

All measurements (except the Cary spectrophotometer readings) were recorded digitally on paper tape for computer analysis. In the temperature region of interest, the time interval between data points was 4 sec.

D. Irradiation

The irradiations were performed in a 10 000-Ci γ cell. The Co^{60} source was placed near the windowless side of the sample chamber, which had a wall thickness of 0.75 mm. The irradiation dose was varied over more than 4 orders of magnitude by varying the distances between the center of the tail and the source from 20 to 150 cm and the exposure times between 1 min and 10 h. The attenuation due to the material of the cryostat tail could be estimated. The highest applied dosage was estimated to be 10^6 rad corresponding to a calculated energy deposition of 1.8×10^{20} eV/cm^3.

E. Sample Treatment and Experimental Procedures

The KBr single crystals of the desired sizes were purchased from Harshaw Chemical Co. Before mounting they were annealed at approximately 300 °C for several hours and allowed to cool down slowly. This treatment was repeated before several experimental runs, healing out all radiation-induced damage. A simpler procedure, not involving the opening of the cryostat, was to anneal the crystals at room temperature. This procedure removed at least 90% of the F-center concentration produced at 10 °K. No F-aggregate or V bands remained.

In a series of runs the samples were annealed only at 35 °K before each reirradiation, allowing the defects stable at a higher temperature to accumulate. This permitted the study of their influence on the low-temperature annealing data.

III. RESULTS AND DISCUSSION

A. Thermally Stimulated Luminescence and Conductivity

In the temperature regions considered (< 35 °K) the TSC and TSL show similar (though not identical) behavior with respect to their dependence on temperature and on irradiation dose (Fig. 2). Moreover, the identical outputs of the filtered and unfiltered luminescence indicate that its spectral composition did not change. For the annealing runs shown in Fig. 2, the crystals had been previously exposed to a radiation dose of approximately 2×10^{18} eV/cm^3 and subsequently annealed at 35 °K. The γ irradiation was applied consistently at 10 °K. Five annealing peaks could be distinguished, as can be seen clearly from the Arrhenius plot in Fig. 3. The peaks are also listed in Table I. The activation energies were obtained from computer fits to the rising edge of the peaks. The characteristics of the data with respect to varying irradiation dosages suggest a separate discussion of the "principal peak" appearing at 27 °K, and the remaining "low-temperature peaks." The TSL of the former peak grows linearly with dose (Fig. 4), while the other peaks seem to saturate after an irradiation dose of 2000 rad (3.6×10^{17} eV/cm^3). The ratio between TSL maxima of the 24° peak and of the principal peak is plotted versus the dosage in Fig. 5. This dependency can be reasonably well described by the expression $(1+R/R_0)^{-1}$, where R is the irradiation dose and $R_0=3.6\times10^{17}$ eV/cm^3. It should be noted that this relationship is more reproducible than the absolute peak intensity as a function of dose. The same relationship can be established for the ratio of all low-temperature peaks with the principal peak, with the proper choice of a proportionality constant. The ratios of the TSC peaks lead to very similar relations.

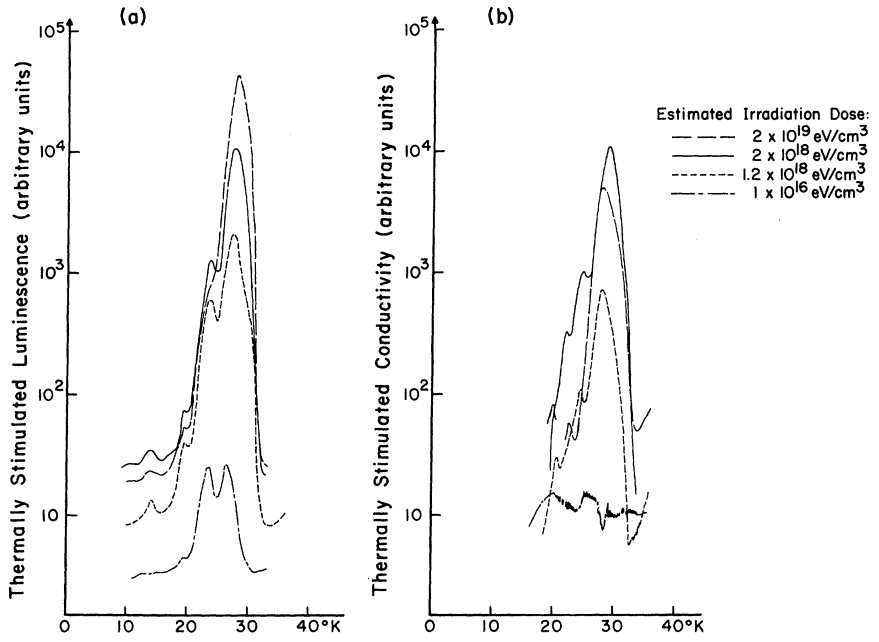

FIG. 2. (a) TSL and (b) TSC of KBr γ-irradiated at 10 °K after four different irradiation doses. Before each run the crystals were annealed at 35 °K.

B. Low-Temperature Peaks

The low-temperature peaks are rather small in intensity. If some of these peaks were due to an ionic motion in a random walk process they should be several orders of magnitude larger, according to our estimates.[5] The simultaneous appearance of conductivity and luminescence would rather suggest that the signals are caused by electronic processes. In such a process electrons would be raised into the conduction band during annealing; their subsequent trapping would give rise to a photon emission. For high irradiation doses the number of conduction electrons produced during the time period of the 24° peak is approximately $10^{13}/cm^3$.

At 22 °K a conductivity peak is recognizable, which is not accompanied by a corresponding luminescence signal. A better resolution was obtained in an annealing run with a heating rate 0.0023 °K sec^{-1}, i.e., approximately $\frac{1}{4}$ of the standard rate. The temperature of irradiation for this particular run was 17 °K with a dose of 4.8×10^{19} eV/cm^3 (see Fig. 6). This peak at 22 °K may be due to an ionic conductivity, though it is very small. The temperature location and peak magnitude are consistent with the kinetic data obtained by Itoh *et al.*[1]

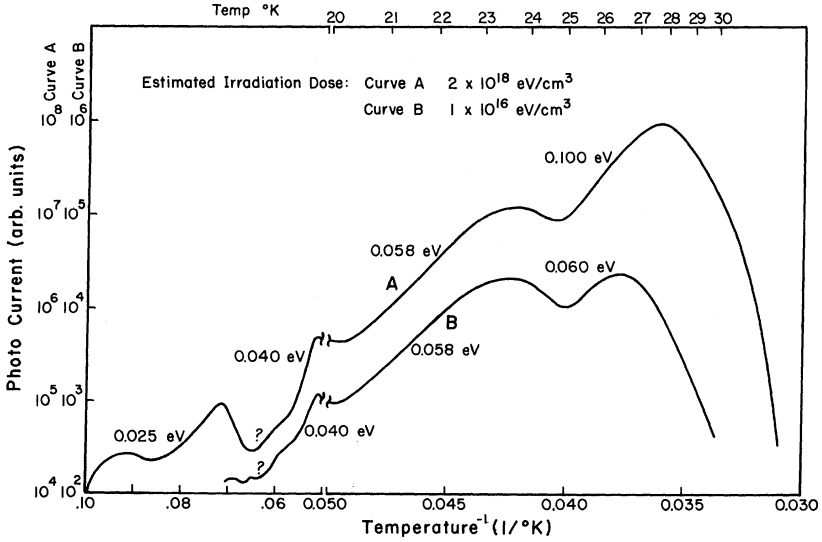

FIG. 3. Arrhenius plot of the TSL during isochronal annealing. Irradiation temperature 10 °K.

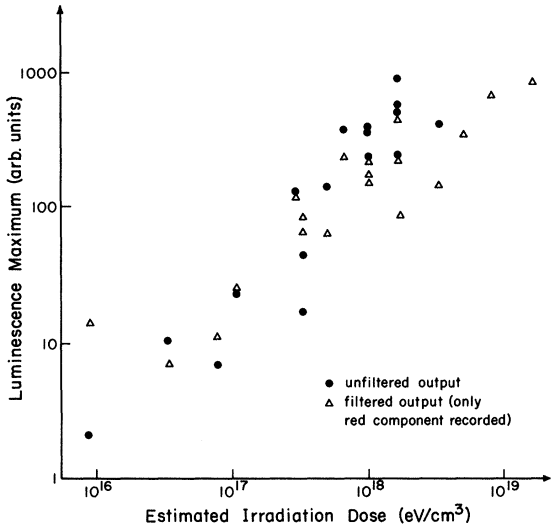

FIG. 4. Maximum of the 27 °K luminescence peak versus irradiation dose in KBr. Irradiation temperature 10 °K.

C. Principal Peak

It was mentioned that the principal peak of the TSL grows linearly with irradiation dose. The conductivity signal shows signs of saturation above a maximum conductivity of 10^{-14} Ω^{-1} cm^{-1}; the maximum was reached in a virgin crystal after an irradiation dose of 10^4 rad (1.8×10^{18} eV/cm^3). Apart from their relative magnitudes, the shapes of the TSC and TSL are identical within the experimental limits for each individual run. But the peak shape exhibits a continuous change with varying irradiation dose. The most pronounced feature is that the activation energy obtained by curve fitting as well as by a leading edge analysis varies from 0.060 eV at low doses to 0.100 eV at higher doses [Fig. 7(a)].

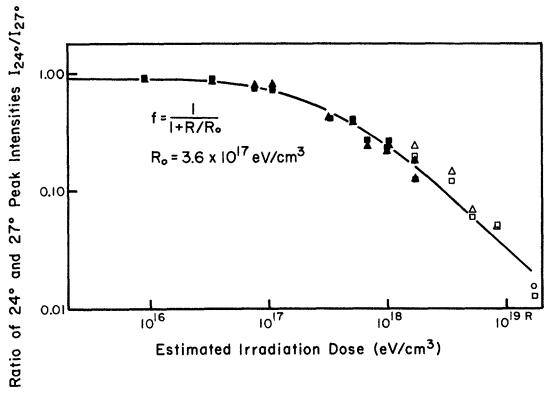

FIG. 5. Ratio of the luminescence peak intensities of the 24° peak and the 27° peak versus irradiation dose. The solid line represents the function $1/(1+R/R_0)$.

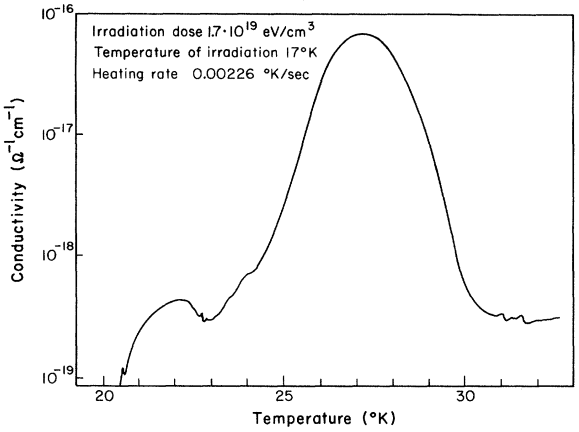

FIG. 6. TSC of KBr γ-irradiated at 17 °K, irradiation dose 1.7×10^{19} eV/cm^3, heating rate 0.002 °K/sec.

The temperature of the peak maximum also depends on the radiation dose, but only very slightly [Fig. 7(b)]. At low dosages it rises monotonically with increasing dose, but it remains at 27.5 °K above a moderate radiation dose of approximately 10^{17} eV/cm^3.

It cannot be uniquely determined whether the conductivity is of electronic or ionic nature, but the close similarity between the TSL and TSC curves suggests an electronic current. For this case the TSL and TSC signals are proportional to each other regardless whether the photon is emitted during the release of the electron or during its recombination with a trap. It is assumed that the electronic Schubweg remains constant during the time period of the annealing peak. In previous papers[3,5] it has been pointed out that in the case of a first-order kinetics the ionic and electronic currents behave identically, but it is shown below that for the principal peak a simple first-order kinetics does not apply.

The conductivity σ may then be expressed by

TABLE I. Annealing maxima for thermally stimulated conductivity and luninescence occurring below 30 °K in KBr γ-irradiated at 10 °K.

Temperature (°K)	Activation energy (eV)	Pre-exponential factor (sec^{-1})	Order of reaction
14	0.025	1.5×10^{7}	1
17	?	?	?
20	0.040	2.0×10^{8}	1
24[a]	0.058	2.0×10^{10}	1
27	0.060 to 0.105	1.5×10^{10} to 4 $\times10^{16}$	Not unique

[a]Maximum at 22 °K was observed for the conductivity only.

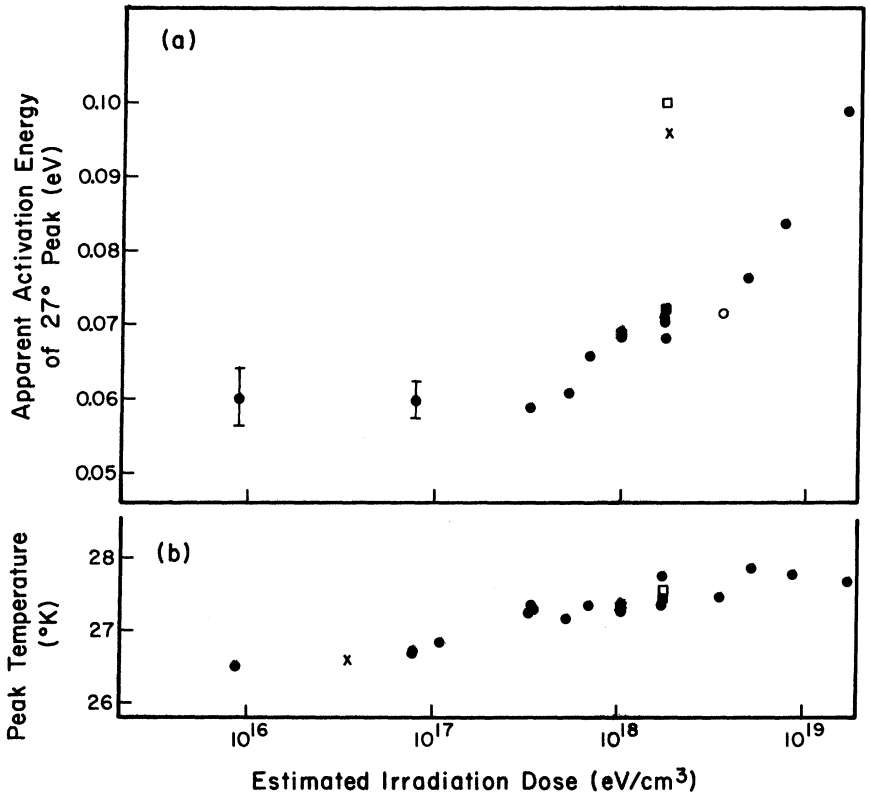

FIG. 7. (a) Apparent activation energy of the principal peak and (b) temperature of peak maximum versus irradiation dose. Pretreatment of the crystals: x annealed at 300 °C, □ irradiated with 1.6×10^{18} eV/cm^3 and subsequently annealed at room temperature, ■ irradiated with 2.5×10^{19} eV/cm^3 and subsequently annealed at room temperature, ● irradiated with $>1.6\times10^{18}$ eV/cm^3 and subsequently annealed at 35 °K.

$$\sigma = \gamma e \omega_0 \left(-\frac{dn}{dt}\right)_{\mathrm{Rec}}, \qquad (1)$$

where $(-dn/dt)_{\mathrm{Rec}}$ is the rate at which the defects annihilate by recombination. e is the electronic charge and ω_0 is the electronic Schubweg per unit field strength; γ is a yield factor representing the average number of electrons released per recombination event. The electronic Schubweg measured,[6] for nominally pure KBr, is 1.31×10^{-8} cm^2/V. Thus, assuming $\gamma = 1$ the number of electrons released was 1.3×10^{14} cm^{-3} for a dosage of 1.8×10^{18} eV/cm^3. The F-center density produced by this radiation dose was measured optically to be 1.35×10^{15} cm^{-3}.

The saturation of the TSC at higher irradiation doses may be correlated to a growing concentration of electron traps. At low-irradiation doses the residual traps in the original crystals are predominant in determining the electronic Schubweg. At higher doses, the radiation-induced traps become prevalent, the Schubweg shortens, approaching an inverse proportionality with the defect concentration.[7] This effect is also demonstrated in a series of experimental runs, in which the crystal was annealed only at 35 °K before each reirradiation. This low-temperature annealing removed all defects giving rise to the annealing peaks below 35 °K of the TSL and TSC, but the number of trapping centers accumulated, thus shortening the Schubweg. Figure 8 indicates this behavior, where the maximum conductivity signal divided by the irradiation dose is plotted versus the accumulated irradiation dose since the last room-temperature annealing.

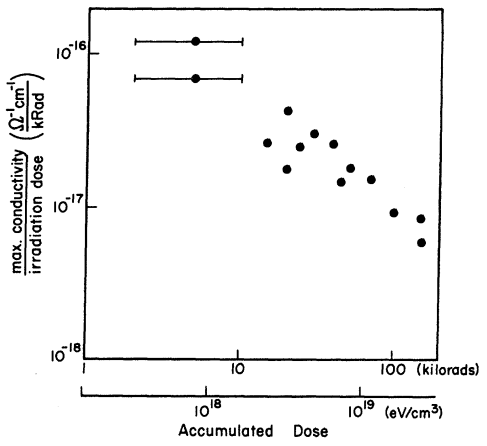

FIG. 8. The efficiency of the TSC production (i.e., the ratio of the conductivity maximum of the 27° peak and the irradiation dose) versus the total dose accumulated since the last annealing at room temperature or higher.

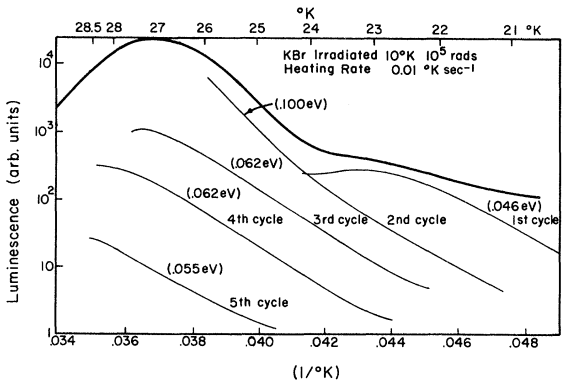

FIG. 9. Luminescence data from thermal cycling versus the inverse temperature; heavy curve: uninterrupted heating; light curve: individual heating cycles.

D. Thermal Cleaning

In an attempt to separate processes controlled by different activation energies, thermal cleaning experiments were carried out. The crystal was heated at the usual rate, but during the early part of the peak the heating was stopped and the crystal was recooled. This means only a small portion of the defects were annealed. The crystal was then reheated to a somewhat higher temperature and again recooled. This was repeated several times. Nichols and Woods[8] described this procedure in detail. The result of the thermal cleaning experiment is shown in Fig. 9. In order to obtain a better picture of the activation energies involved, the log of the signal is plotted on an inverse temperature scale. The heavy curve represents the TSL during the individual heating cycles. The energies in the graph are determined by the slopes of the curves. It can be seen that the principal peak initially involves processes with an apparent energy of 0.100 eV, and after their depletion mostly events with 0.062 eV occur. In addition, with increasing depletion of the centers the peak temperature is moved to higher values. The total time integral under the cycling curves is within 20% equal to the time integral under the curve of the uninterrupted annealing run. This indicates that no retrapping has occurred. A similar experiment was carried out at a dosage of 2000 rad (3.4×10^{17} eV/cm^3), where the leading edge slope corresponds to an energy of 0.06 eV. Except for the absence of the high-energy component, a similar behavior was observed. These data indicate that there are at least two distinguishable annealing processes contributing to the peak at 27 °K.

E. Optical Absorption

The changes in the optical absorption between 250 and 800 nm were investigated by repeated scanning in a sample irradiated to a dosage of 10^5 rad (producing an F-center density of 1×10^{16} cm^{-3}). The optical density at four successively higher temperatures during the experiment is shown in Fig. 10. The over-all behavior was in qualitative agreement with work reported in the literature.[9–11] The F and the composite H band bleached by 20 and 25%, respectively, at 27 °K. The wavelength of the maximum of the H band and the shape of the peak underwent no significant change over this annealing interval. There was a significant reduction in the background of the red side of the H band due partly to annealing of a contribution from the tail of the K band. Some bleaching of both the F' band and the K band is visible. The small bands at 260 and 280 nm, which are believed to be due to impurities, were not affected by the anneal. The I band at 230 nm was also detected in an 2-mm-thick sample irradiated under similar conditions. The band decayed at about 22 °K; however, the variation in the background absorption with rising

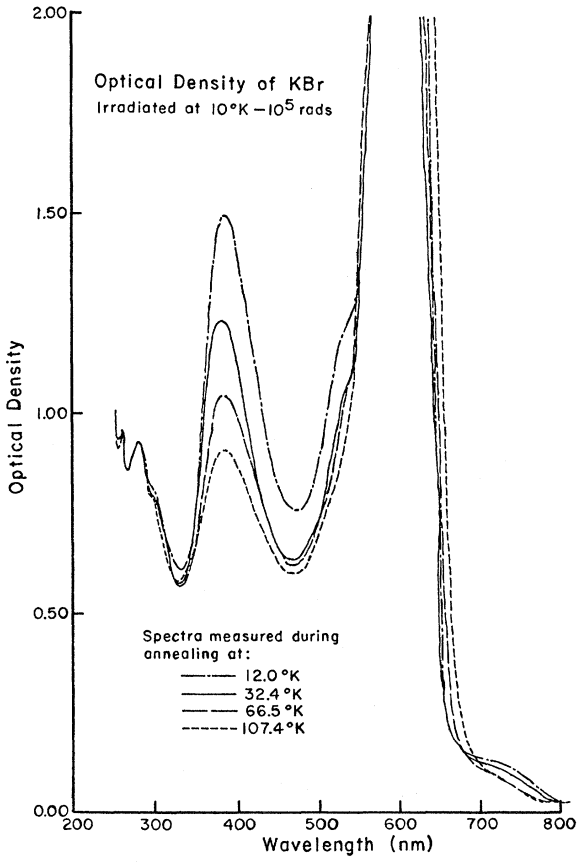

FIG. 10. Absorption spectra of KBr at various stages during isochronal annealing. Irradiation conditions: dose 1.8×10^{19} eV/cm^3, temperature 10 °K.

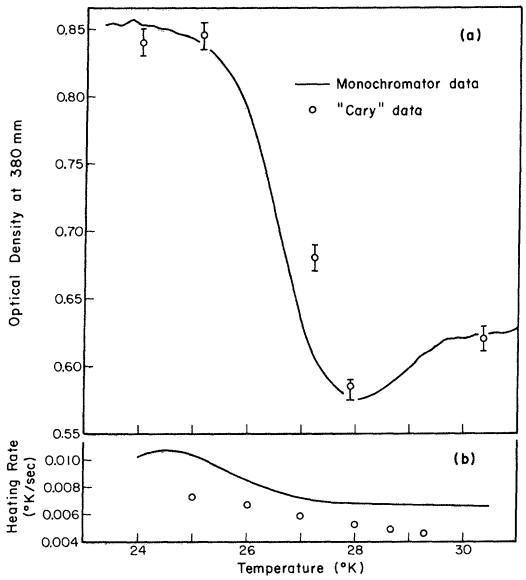

FIG. 11. (a) Optical density at 380 nm and (b) heating rate versus temperature during annealing. Curve: monchromator data; points: "Cary" data, irradiation conditions the same as in Fig. 10.

temperature prevented an exact determination of the bleaching temperature of this band.

The isochronal annealing of the absorption at 380 nm measured with the monochromator system is shown by the solid line in Fig. 11. The points show the data obtained during the scanning experiment discussed above. The heating rates during the anneals are shown below the absorption data. The temperature of the inflection point in the data obtained by differentiation is 26.35 °K. Above 28 °K there was a slight rise in the absorption peaking at 38 °K followed by two further annealing steps at 40 °K and 50 °K. A three-step annealing behavior in the absorption at 380 nm was previously reported by Cape and Jacobs.[10] However, the ratio of the magnitudes of the three steps were different, being for increasing temperature 1 : 0.36 : 0.34 in the present work and 1 : 1.6 : 0.2 in the previous study. The origin of the implied variation in the admixtures of V_I and V_k contribution to the composite band as a function of dosage was not investigated.

Comparison of the temperature of the inflection of the H center annealing with the peak in the luminescence or conductivity data indicated that the two processes were not exactly simultaneous. The H-center bleaching preceded the luminescence peak by 1°. This difference in the peak temperature could not be ascribed to temperature lags within the system. The possibility of a luminescence contribution to the intensity of the transmitted light was found to be negligible. If a maximum luminescence contribution equal to 15% of the transmitted intensity at 28 °K was subtracted the corrected absorption curve would inflect at 27 °K, but the minimum in the absorption shown in Fig. 11 is removed. The slope of the annealing curve was slightly increased. Thus, in view of the similarity of the data runs shown in Fig. 11, we believe that any luminescence contribution is small, and that there is a real difference between the annealing temperatures of the absorption on one hand and the luminescence and conductivity on the other hand.

The analysis of the annealing curve showed that the leading edge corresponded to an activation energy of 0.097 eV. Above the inflection point uncertainties in the background prevent an analysis of the kinetics.

F. Analysis

A mathematical analysis of the annealing data showed that the events governing the annealing behavior in the 25–30 °K region cannot be described by a conventional first- or second-order kinetics. In the absence of a model upon which to base the annealing kinetics, attempts were made to fit the experimental data to a kinetic equation of a more general form, where the concentration of traps may be varied arbitrarily. In particular, the data for various dosages were analyzed using distributions of activation energy and rate constant, and considering the peak to arise from sequential and/or superimposed annealing events. The formulations represent a wide range of physical situations involving dissociation effects and lattice recombination processes. [Although it has not been possible to distinguish the initiating process(es), our experimental results on the dosage and reexcition behavior combined with the results by other workers indicate that the annealing process(es) at 27 °K involves ionic recombination. However, the observed current is mostly or completely of electronic origin.]

The equation for annealing kinetics of point defects in which a variation in the number of traps is taken into account may be described by

$$-\frac{dn}{dt} = nn_R K \exp(-E/kT), \tag{2}$$

where n and n_R are the concentrations of the radiation defects and of the recombination centers, respectively. E is the activation energy controlling the process, and K is a rate constant corresponding to a second-order frequency factor. n_R may be a constant, corresponding to a pure first-order kinetics. However, in most cases the recombination centers will be annihilated during the anneal. Therefore,

$$n_R = n' + n, \tag{3}$$

where n' is the concentration of remaining recombination centers after the complete annealing of the defects. A plot of the ratio

$$-\frac{dn}{dt}\Big/ nn_R \tag{4}$$

on a semilogarithmic scale versus $1/T$ should give a straight line according to Eq. (2), with a slope determined by the activation energy. Since the signals of both the TSL and TSC (if it is of electronic nature) are proportional to the rate of decay, this ratio can be expressed in terms of the observed signals and their time integrals. For the quantity n_R the relation (3) was applied. For practical reasons n' was expressed by a parameter

$$\rho = n'/n_0 , \tag{5}$$

where n_0 is the initial concentration of defects, which is proportional to the integral of the signal over the whole peak.

Attempts to fit the principal peak of the luminescence by superposing a series of monomolecular peaks (n_R = const) with energies of 0.100 and 0.060 eV proved unsatisfactory. The increase in the width of the peak with increasing dosage could not be fitted using a systematic variation of either K or E. Moreover, the frequency factor corresponding to the 0.100-eV activation energy is unreasonably high (10^{17} sec^{-1}), although the energy is in reasonable agreement with theoretical estimates of the thermal motion of the H center.[12]

The curves were then analyzed according to Eq. (2), in which ρ was a variable parameter. In Fig. 12 plots of the derivative of the log of expression (4) are shown for various values of ρ applied on two typical runs, one with a moderate irradiation dose (2×10^3 rad) and one with a higher dose (10^5 rad). The scale of the ordinates indicates the corresponding activation energy. It can be seen that only for lower irradiation dosages [Fig. 12(a)] a unique activation energy can be obtained (0.062 ± 0.003 eV), in which case the parameter ρ has to be chosen rather small (~ 0.10). The curve for $\rho = 0$ corresponds to a pure second-order kinetics. We see that only a slight difference between the number of defects and that of the trapping centers

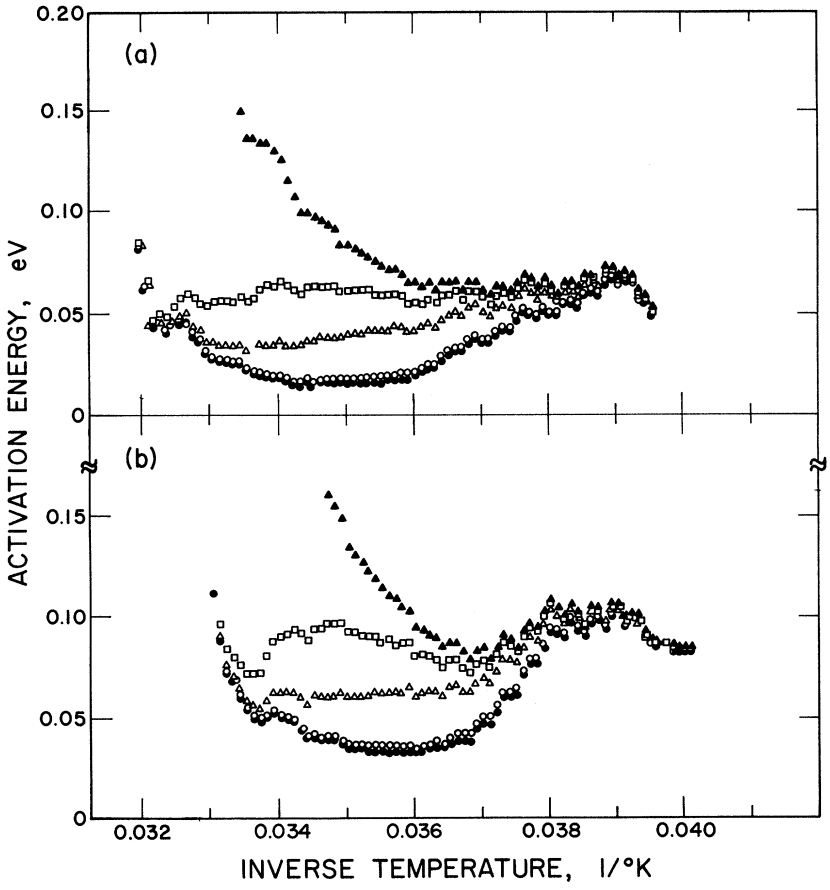

FIG. 12. Determination of activation energy E as a function of temperature for various values of ρ, where $E = -k(d/dT^{-1}) \ln[\Delta n/n(n+pn_0)]$. Curve (a) 2×10^3 rad (3.6×10^{17} eV/cm^3). Curve (b) 1×10^5 rad (1.8×10^{19} eV/cm^3). ●: $\rho = 20$, ○: $\rho = 5.0$, △: $\rho = 0.4$, □: $\rho = 0.1$, ▲: $\rho = 0.0$.

alters appreciably the rate of annealing at the trailing edge. For intermediate doses a satisfactory straight line is found, but with a decreasing ρ; E again is ≈ 0.062 eV.

For the cases of higher irradiation dosages a constant slope cannot be obtained by this analysis. However, for larger ρ, i.e., by approaching a pure first-order kinetics, two steps can be distinguished [Fig. 12(b)]: The leading edge exhibits an energy of 0.100 ± 0.005 eV, and in the approximate temperature region of the peak maximum the slope changes suddenly corresponding to a much lower energy of ≈ 0.035 eV . The leading-edge slope agrees with the activation energy obtained from the optical-absorption data. Processes governed by 0.060 eV appear to be buried under the higher-energy process during the initial stage of the annealing.

IV. CONCLUDING REMARKS

The evidence of this study supports the view that the observed annealing processes involve the recombination of lattice defects. The magnitude of the thermally stimulated luminescence peak at 27 °K was characteristic of irradiation dosage alone and not dependent on the irradiation history or on previous thermal treatment. Such behavior is characteristic of the growth of color centers at low temperatures, and therefore, the authors have attempted to interpret the data in terms of the recombination of Frenkel defects.

Since it was impossible to reexcite the peaks optically and in view of the proximity of the temperatures at the observed annealing processes to temperatures where interstitial-type centers are known to anneal, it appears unlikely that any of the effects are caused by the dissociation of a complex electron trap. However, the behavior of the conductivity with accummulated radiation dosage indicated that the conductivity was due to the motion of electrons. These may be freed during an interstitial-recombination event. A production of conduction electrons due to the luminescence output is unlikely because at temperatures between 30 and 50 °K luminescence peaks are not accompanied by conductivity.

The thermal-cleaning experiment and the variation of the activation energy from the leading edge with dosage suggest that the peak at 27 °K may be due to two overlapping processes. One process was visible at low dosages and after the cleaning of the high-dosage data, and was characterized by an energy of 0.06 eV. The other process was characterized activation energy of 0.10 eV and has been correlated to the annealing of the optical absorption. The present optical data are not sufficiently accurate to exclude a correlation with the 0.06-eV process. Further experimental work with higher H-center densities is clearly required. At low dosages the H-center absorption peak could not be sufficiently well resolved to yield reliable kinetics data.

A tentative model has been advanced for the low-energy process based on the correlation with the energy observed by Itoh *et al.*[1] The kinetics of the annihilation for various dosages can be understood if it is assured that the trapping-center concentration was relatively unaffected by the irradiation dosage. Thus, at the lowest dosages the peak had an almost monomolecular form. With dosage increase the peak broadens at the high-temperature side and the curve could be fitted with a small value of ρ [Eq. (5)] corresponding to mixed kinetics. This model is consistent with the thermal-cycling experiment, which was carried out both at high and intermediate dosages, and showed a progressive increase in the peak temperature with successive cycles.

The kinetics of the high-energy process, which appears to involve the H- and F-center recombination, is not understood. If the H center diffuses with an energy of 0.10 eV by an interstitialcy mechanism, which is in fair agreement with the calculations of Dienes *et al.*,[12] it is difficult to explain the high rate constant on the basis of any reasonable thermal-trapping cross section. A similar energy but a lower and more reasonable rate constant for the diffusion has been observed by Ueta.[13] In order to fit the slope of the high-dosage data we introduced a model involving two sequential monomolecular processes: The initial process is the dissociation of the H center into a V_k center and an interstitial, which then diffuses to annihilate at an F center. The annihilation process following the H-center decomposition results in the luminescence and possibly the production of a free electron. Since in the early stage of the H-center dissociation the production of interstitials will follow the functional behavior of $e^{-E_H/kT}$, E_H being the dissociation energy of the H center, the signal of the luminescence and electronic conductivity would be proportional to $e^{-E_H/kT} e^{-E_i/kT}$, where E_i is the migration energy of the interstitial. This means the sum $E_H + E_i$ would determine the initial activation energy for this type of process. In the final stage only the migration energy of the interstitial E_i would be significant. In order to explain the absence of ionic currents and the low activation energy (0.035 eV) of the secondary process we have to assume that the interstitial–F-center recombination occurs in localized regions, and the small magnitude of the conductivity would require that most ($\sim 90\%$) of the excess electrons from the lattice-recombination events recombine with the V_K centers by tunneling rather than via the con-

duction band.

The authors feel that the study of low-temperature luminescence and conductivity is demonstrated to be a useful tool for studying irradiation-induced defects in KBr. Further work at high dosages is clearly required.

ACKNOWLEDGMENTS

This work was supported by the U. S. Atomic Energy Commission, with additional support by the Advanced Research Projects Agency through the Materials Science Center at Cornell University.

The authors wish to thank Professor Smoluchowski and Professor Royce, as well as Professor Silsbee for useful discussions. A. W. Haberl assisted during the experiments and was mainly responsible for the data processing at the Cornell Computing Center.

*Present address: U. S. Bureau of Mines, Pittsburgh, Pa. 15213.

†Present address: Argonne National Laboratory, Argonne, Ill. 60439

[1]N. Itoh, B. S. H. Royce, and R. Smoluchowski, Phys. Rev. 137, A1010 (1965).

[2]N. Itoh, B. S. H. Royce, and R. Smoluchowski, Phys. Rev. 138, A1766 (1965).

[3]A. Taylor, Phys. Status Solidi 37, 401 (1970).

[4]D. Dutton and R. Maurer, Phys. Rev. 90, 127 (1953).

[5]W. Fuchs and A. Taylor, Phys. Status Solidi 38, 771 (1970).

[6]G. R. Hugget and K. Teegarden, Phys. Rev. 141, 797 (1967).

[7]R. W. Pohl, Proc. Phys. Soc. 49, 3 (1937).

[8]K. H. Nichols and J. Woods, Brit. J. Appl. Phys. 15, 783 (1964).

[9]H. Rüchardt, Phys. Rev. 103, 873 (1956).

[10]J. S. Cape and G. Jacobs, Phys. Rev. 118, 966 (1960).

[11]R. Balzer, H. Peisl, and W. Waidelich, Phys. Status Solidi 31, K29 (1969).

[12]G. F. Dienes, R. D. Hatcher, and R. Smoluchowski, Phys. Rev. 157, 692 (1967).

[13]M. Ueta, J. Phys. Soc. Japan 23, 1265 (1967).

PHYSICAL REVIEW B VOLUME 2, NUMBER 8 15 OCTOBER 1970

Distortion and Polarization near Color Centers*

A. M. Stoneham†

Physics Department and Coordinated Science Laboratory, University of Illinois at Champaign, Urbana, Illinois‡

and

R. H. Bartram

Physics Department, University of Connecticut, Storrs, Connecticut

(Received 26 March 1970)

A general method is presented for calculating the static polarization and distortion near a defect. It assumes that the lattice responds to the average, but consistently chosen, charge distribution of the electrons associated with the defect, and uses the shell model to describe the lattice dynamic and dielectric properties of the host. The lattice is discrete, without continuum approximations; there are no artificial restrictions on the range of the distortion, and asymmetric distortions, as from the Jahn-Teller (JT) effect, are included. The variation of the electronic wave function as the lattice distorts may be included consistently even in cases where there is mixing of nearby levels. The method is illustrated by a calculation for the $2p$ excited state of the F center in KBr. It proves necessary to include the ion-size terms in the interaction of the defect electron with the lattice. The results are sensitive to the detailed model chosen for the lattice dynamics. However, certain features, such as the outward motion of the nearest neighbors, the JT distortion, usually tetragonal, and the substantial energy lowering, typically 0.5 eV, are common to these models.

I. INTRODUCTION

One of the central problems in color-center theory is the question of the polarization and distortion of the host lattice, and the dependence of these on the electronic state. Accurate calculations of transition energies and, more particularly, the Stokes shift and bandwidths are very sensitive to the model used. We shall show that these questions can be dealt with systematically in the Hartree limit, in which the lattice responds to the average, but consistently calculated, charge distribution of the defect electron, and using a model such as the shell model to describe the lattice dynamics of the host. The method can be used for many centers, including the F center and the V_k center, and can be extended